Received: 22 December 2022 | Accepted: 10 January 2023 | Published on: 28 February 2023

DOI: 10.1002/asna.20220128

Astronomische Nachrichten

PROCEEDING

Searching for overlooked TDEs in the 4XMM catalogue

Andrea Sacchi[1,2] | **Guido Risaliti**[1,3] | **Giovanni Miniutti**[4]

[1]Dipartimento di Fisica e Astronomia, Università degli Studi di Firenze, Sesto Fiorentino, Italy

[2]Instituto de Fìsica de Cantabria, CSIC-U, Cantabria, Santander, Spain

[3]Osservatorio Astrofisico di Arcetri, INAF, Florence, Italy

[4]Departamento de Astrofisica, Centro de Astrobiologìa (CSIC-INTA), Villanueva de la Cañada, Spain

Correspondence
Andrea Sacchi, IFCA, Av. de los Castros, Cantabria, Santander 39005, Italy.
Email: andrea.sacchi@unifi.it

Abstract

Tidal disruption events (TDEs) are usually discovered as bright transients, either in the X-ray or optical/UV band. These events are often characterized by a “super-soft” emission in the X-ray band, which has not been observed in any other extragalactic source, with few exceptions (novae and supersoft active galactic nuclei, AGN), which can however be distinguished by their optical behavior. By cross-correlating optical and X-ray catalogs and filtering for extremely steep (photon index $\Gamma > 3$) and highly luminous ($L_X > 10^{41}$ erg s^{-1}) objects in external galaxies nuclear regions, we aim to detect overlooked TDEs. With our blind search, we retrieved about 60 sources. Among these, 36 sources show steeper-than-usual spectra, but, with their optical classification, can be considered standard AGNs. Instead, fifteen are well-studied supersoft AGNs or TDEs, demonstrating the efficiency of our selection. The remaining 9, are previously unknown sources. Five are extremely soft-excess dominated AGNs, while 4 sources are optima TDE candidates. In this work, we focus on these 4 latter sources.

KEYWORDS

black hole physics, galaxies: Nuclei, galaxy: Center

1 | INTRODUCTION

Traditionally, supersoft X-ray sources (SSSs) are associated with cataclysmic events (novae) due to mass transfer phenomena onto white dwarfs. However, these are not the only known or most intriguing SSSs: extragalactic objects can sometimes exhibit supersoft X-ray spectra coupled with high luminosities. In this category often fall ultra-luminous X-ray sources (ULXs) (Kaaret et al. 2017), supersoft AGNs (Miniutti et al. 2019; Terashima et al. 2012), and tidal disruption events (TDEs) (Saxton et al. 2020).

Ultraluminous X-ray sources (ULXs) and hyperluminous X-ray sources (HLXs) are defined as off-nuclear X-ray objects with luminosities exceeding 10^{39} erg s^{-1} and 10^{41} erg s^{-1}. The latter sources are of particular interest given the fact that they represent the most convincing candidates for intermediate-mass black hole (IMBH) candidates (e.g., Farrell et al. 2009).

Supersoft AGNs are peculiar sources discovered in recent years. 2XMM J123103.2+110648 (Terashima et al. 2012), GSN 069 (Miniutti et al. 2013), and RX J1301.9+2747 (Sun et al. 2013), show a similar behavior: these sources are optically classified as Seyfert 2 galaxies but exhibit a super-soft X-ray spectrum with strong variability. 2XMM J123103.2+110648 is associated with a ~ 3.8-hr periodicity (Lin et al. 2013), while the two latter sources show peculiar recurrent flares in the form of quasi-periodic eruptions (QPEs) (Giustini et al. 2020; Miniutti et al. 2019). It is to be noted that for both sources, a TDE scenario has been invoked to account for the lack of broad optical emission lines and the long-term decay in flux of GSN 069 (Lin et al. 2017).

TDEs are extreme variability transients occurring at the disruption of a star by a supermassive black hole (SMBH). When the tidal forces of the hole overcome the stellar self-gravity, the star gets torn apart and its debris gets partly accreted, generating bright electromagnetic emission (Phinney 1989; Rees 1988). The time scales (days and months) on which these events evolve offer unique opportunities to investigate accretion phenomena and probe the properties of otherwise quiescent (SMBHs). The X-ray spectrum of a TDE is usually dominated by the emission of the optically thick accretion disc formed by the stellar debris around the SMBH. Its appearance is that of a cold blackbody with temperatures below 100 eV (Saxton et al. 2020).

TDEs are usually detected thanks to their extreme variability. This method, employed by today's facilities, which can repeatedly scan the sky looking for transients, is an extremely efficient way of detecting new events. It is likely, though, that there are TDEs hiding in the available catalogs and archives, being spotted by chance but not yet recognized.

Here, we present four sources selected by cross-matching X-ray and optical catalogue and selecting super soft, highly luminous sources in the nuclear regions of their host galaxies. These sources are the most convincing candidate for TDEs.

2 | SOURCE SELECTION

We started by taking the more than 8×10^5 detections of the XMM-Newton catalog of serendipitous sources (4XMM-DR9, Webb et al. 2020), and we computed (i) the signal to noise ratios in the ultrasoft 0.2–0.5 keV (SNR_1) and soft 0.5–1 keV (SNR_2) bands, as well as (ii) the photon index Γ_{21} for the ultrasoft to soft band and that for the soft to medium (1–2 keV) band, Γ_{32}. In order to obtain SSS with good signal to noise, we selected all the point-like objects having a high signal-to-noise ratio in both the ultrasoft and soft band ($SNR_1 > 7$, $SNR_2 > 3$) and a steep photon index in the ultrasoft band ($\Gamma_{21} > 3$). As this criterion allows for little to no absorption (even compared with the average Galactic level), we also selected the sources with high signal to noise ratio and steep photon index in the sole soft bands ($SNR_2 > 7$, $\Gamma_{32} > 3$), but with an additional constraint on the photon index in the ultrasoft band ($\Gamma_{21} > -1$) to avoid star-forming regions and the most heavily obscured AGNs, dominated by thermal/photo-ionized plasma emission in the soft X-ray band.

Then, we retrieved redshift information for as many sources as possible by cross-matching our sample with the available galaxy catalogs in SIMBAD, the largest one being SDSS DR16 (Ahumada et al. 2019), followed by 2dFGRS (Colless et al. 2003), 6dFGS DR3 (Jones et al. 2009) and LCRS (Shectman et al. 1996). We kept all the matches with an angular distance (measured from the source position provided by the 4XMM-DR9 catalog) smaller than 5 arcsecond. Finally, we required the luminosity in the full 0.2–12 keV X-ray band of the selected galaxies to be larger than 10^{41} erg/sec. This selection process resulted in 61 sources.

One of these, SDSS J123408.85+090542.4, is the brightest cluster galaxy (BCG) of the compact cluster SDSSCGA 1202 (Yoon et al. 2008); this object was promptly eliminated from the sample as the soft X-rays emission is the result of the gas warming in the potential well of the cluster rather than due to accretion phenomena. This is also confirmed by X-ray spectral analysis which reveals that emission by an optically thin, warm gas with fixed solar abundances reproduces the data well.

Out of the remaining 60 sources, 15 are well-known sources characterized by rather extreme X-ray properties in terms of soft spectral emission and variability:

- 8 TDEs or TDE candidates: 2MASX J02491731−0412521 (Esquej et al. 2007), ASASSN-15oi (Holoien et al. 2016), ASASSN-14li (Maksym et al. 2014), 2XMM J123103.2+110648 (Lin et al. 2017), 2MASS J12013602+3003052 (Saxton et al. 2012), SDSS J150052.07+015453.8 (Lin, Guillochon, et al. 2017), GSN 069 (Shu et al. 2018), a super-soft AGN, which produced a huge X-ray burst followed by a long-term decay and also exhibits QPEs, 2MASX J19271951+6533539, a changing look AGN for which the variability is thought to be caused by a TDE (Ricci et al. 2020); 2XMM J141711.0+522541, an off-nuclear transient which could be associated with a TDE onto an IMBH (Lin et al. 2016);
- 7 extreme AGNs, exhibiting exceptional short and/or long-term variability coupled with super-soft spectra: RX J1301 (Giustini et al. 2020), which is associated with QPEs; 2MASX J10343860+3938277, which exhibits a very pronounced soft excess and quasi-periodic oscillations (GierliiIski et al. 2008); the highly variable narrow line Seyfert galaxies 4 U 0708-49 (Boller et al. 2002), 2MASX J13251937−3824524 (Boller et al. 1997) and 2MASX J14062191+2223462 (Mallick & Dewangan 2018); and PHL 1092, an extreme variability example of a weak line, often X-ray weak narrow line quasar (Miniutti et al. 2009).

All these 15 sources fall in the categories described in the introduction and represent, therefore, a reassuring sanity check of the ability to obtain the type of sources

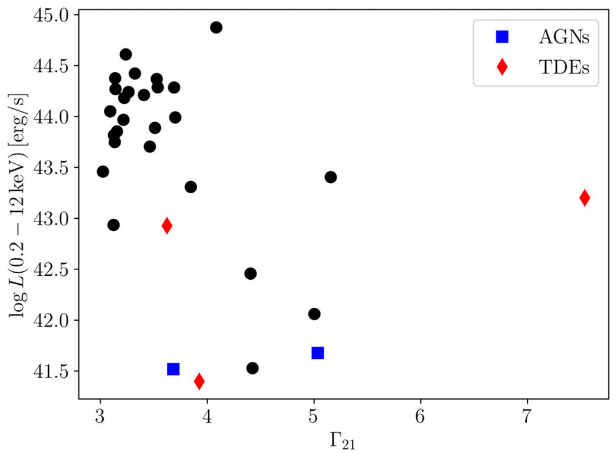

FIGURE 1 The 31 sources brought forth by our selection in the ultrasoft band are shown in the $L_X - \Gamma_{21}$ plane. Blue rectangles and red diamonds show the extreme AGN and TDEs known in literature, respectively.

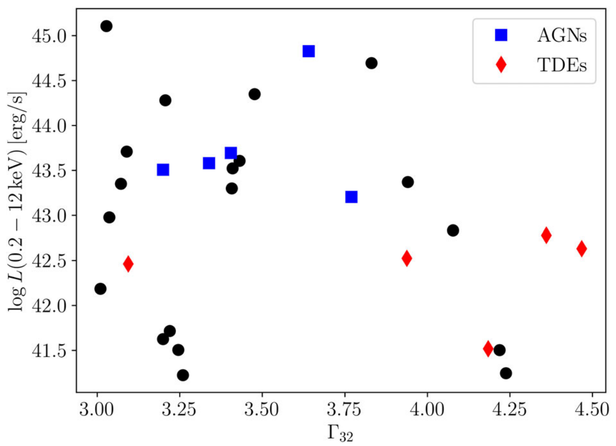

FIGURE 2 The 29 sources brought forth by our selection in the soft band shown in the $L_X - \Gamma_{32}$ plane. Blue rectangles and red diamonds show the extreme AGN and TDEs known in literature, respectively.

we are looking for from our selection criteria. As these 15 sources have all been extensively studied in the X-ray band in the past, we do not discuss them any further.

Figures 1 and 2 show, in the $L_X - \Gamma_{21}$ and $L_X - \Gamma_{32}$ plane, respectively, the 60 selected sources. Figure 1 shows the 31 sources selected in the ultrasoft band, while Figure 2 the 29 retrieved from the soft band selection. The 7 extreme AGNs and 8 TDEs known in literature are highlighted with blue triangles and red diamonds, respectively. The black points represent the remaining 45 sources that are discussed below.

For each observation of the remaining 45 sources, we retrieved the EPIC data from the XMM-Newton science archive and reduced them following the standard procedure. We considered the band between 0.2 and 10 keV for the EPIC PN data and between 0.2 and 7 keV for the MOS data. Data were regrouped in order to have at least one count in each channel (any further rebinning shown in the figures is purely graphical), and we employed the C-statistic for spectral fitting. We used the XSPEC package to analyze the spectra of our sources. We initially adopted a simple model composed by an absorbed blackbody plus powerlaw, redshifted to the source distance (*zTbabs* × *[zBbody + zPowerlw]* in XSPEC) with an additional layer of absorption (*Tbabs*) with column density fixed to the Galactic value.

Out of these sources, we identified:

- 30 sources optically classified as BLAGN (19 by Pâris et al. 2018, 4 by Véron-Cetty & Véron 2010, 3 by Pierre et al. 2016, 2 by Rakshit et al. 2017, 1 by Bär et al. 2017, and 1 by Esquej et al. 2013). Their X-rays emission, although often unusually steep, appears compatible with their optical classification and typically comprises a relatively strong soft excess with $kT \sim 100$–200 eV and a power law emission component dominating the hard energy band. These sources belong to the soft X-ray bright tail of the AGN population, without any other strikingly distinctive properties with respect to "normal" AGN.
- 3 sources optically classified as Seyfert 2 galaxies. NGC 6264, classified by Véron-Cetty & Véron 2010, is a well-known Compton-thick AGN hosting an H_2O megamaser (Castangia et al. 2013). 2dFGRS TGS243Z047 is classified as a heavily obscured AGN by Lacy et al. (2013). 2MASX J10181928+3722419 instead, classified by Toba et al. 2014, has its soft X-ray emission dominated by star formation rather than nuclear activity (LaMassa et al. 2012).
- 2 star formation dominated sources: 2XMM J021704.5−050214, classified as an elusive AGN with star-forming activity (Menzel et al. 2016), and 2MASX J17020882+6412210, classified as a star-forming galaxy by Mickaelian et al. (2018). Their soft X-rays emission is in fact consistent with star formation activity rather than accretion;
- 1 source, 2dFGRS TGS431Z029, is classified as non-active galaxy (Lavaux & Hudson 2011) as its optical spectrum does not show any emission line, and has the distinctive X-rays emission of an obscured, possibly Compton-thick AGN.
- 5 sources with an AGN optical classification but peculiar X-ray emission, which will be further addressed by future works.

The remaining 4 sources show peculiar X-ray spectral properties that are not immediately consistent with their optical classification and strongly hint for a TDE origin of

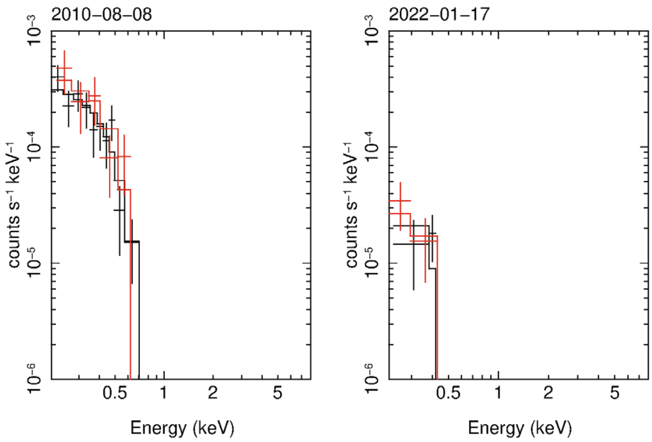

FIGURE 3 X-ray spectra of the source labeled T1. Black data are from the EPIC-pn camera, while red ones are from the EPIC-MOS one.

their emission. These sources will therefore be addressed individually in the following section.

3 | CANDIDATE TDES

Although our tentative classification cannot be considered as unique, the four sources here presented are supersoft, highly luminous sources associated with the nuclear regions of their host galaxies, hence consistent with being TDE candidates. Table 1 resumes the spectral properties described below.

3.1 | SDSS J152717.95+164503.2

This source, labeled T1, has a spectroscopic redshift z = 0.0606 coming from the SDSS DR9 (Ahn et al. 2012), and it is cataloged as a non-active, star-forming galaxy with a star formation rate of $\log \mathrm{SFR} = -0.1192\ M_{\odot}$/year (Toba et al. 2014). It has been observed in August 2010, and its X-rays spectrum is well modeled by a cold blackbody with $kT \sim 60$ eV. We compared this model with a thermal plasma model (*apec*) in order to be sure that the X-ray is not due to star formation. We found that the blackbody model fitted the data significantly better (F-test <3‰). In 2010, the X-ray luminosity between 0.5 and 2 keV of the source was 10^{41} erg/s. We asked for a new observation with XMM-Newton, and the source was reobserved in January 2022 (Proposal ID: 088474, PI: A. Sacchi). After 12 years the spectral shape of the source is unchanged, strongly suggesting that we are still observing the source rather than the host galaxy emission, and its X-ray luminosity dropped by a factor ≈ 20. Its spectrum is shown in Figure 3.

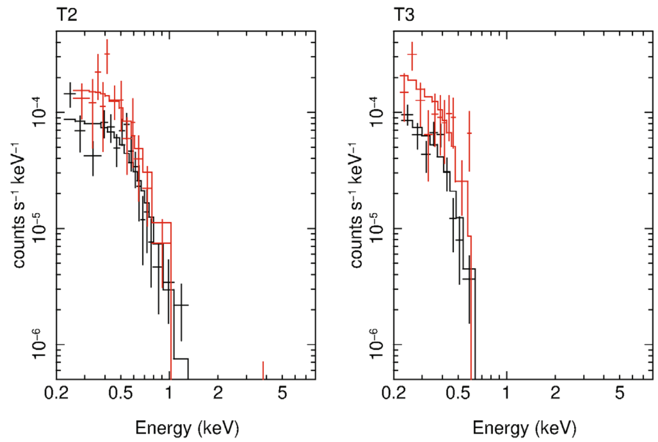

FIGURE 4 X-ray spectra of the sources labeled T2 (left) and T3 (right). The color code is the same as in the previous plots.

3.2 | 2MASX J00414632−2827423

This source, labeled T2, is located at a spectroscopic redshift z = 0.0744 and is identified as a non-active galaxy (Paturel et al. 2003). It has one XMM-Newton observation in which the spectrum is well modeled by a blackbody with $kT = 0.11 \pm 0.01$ keV, and its X-rays luminosity is about 2×10^{41} erg/s. Although the source is located in the outskirt of the Sculptor cluster, its X-rays emission appears to be associated with accretion phenomena rather than with the diffuse cluster emission. In order to test this, we tried modeling the X-ray spectrum of the source with a thermal plasma emission model, but we found that a blackbody can fit the emission of this source significantly better (F-test <2‰). The X-ray spectrum of the source is shown in Figure 4.

3.3 | GAMA 91637

This source, labeled T3, has a spectroscopic redshift z = 0.1775 from the GAMA survey (Driver et al. 2011), and it is cataloged as a non-active galaxy (Liske et al. 2015). It has been observed only once by XMM-Newton, and its X-ray spectrum, shown in Figure 4, is best fitted by a cold blackbody with $kT \sim 60$ eV. The X-rays luminosity for this source is $\sim 4 \times 10^{41}$ erg/s.

3.4 | XXL-AAOmega J234255.95−543001.8

This source, labeled T4, has a spectroscopic redshift z = 0.28633 and it is cataloged as AGN due to the presence of broad emission lines in its optical spectrum (Lidman et al. 2016). It has two XMM-Newton observations, in October 2009 and December 2012. During the first

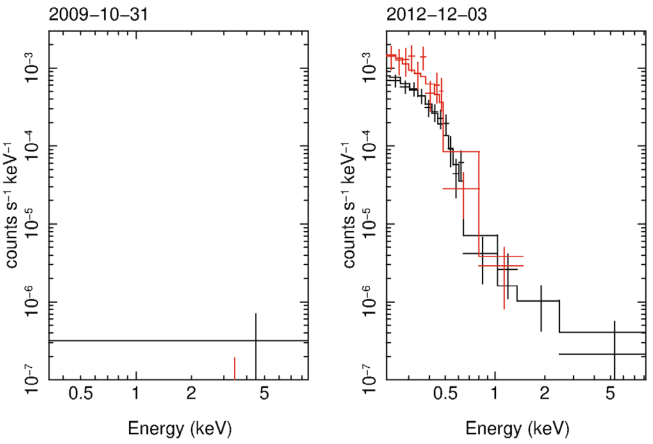

FIGURE 5 X-ray spectra of the source labeled T4. The color code is the same as in the previous plots.

observation, the source was not detected, and the upper limit to its luminosity is $\sim 4 \times 10^{42}$ erg/s. Three years later, the luminosity is almost an order of magnitude larger, $\sim 1.5 \times 10^{43}$ erg/s, and the X-ray spectrum of the source is well modeled by a blackbody with a temperature $kT \sim 80$ eV. The X-rays spectrum of the source is shown in Figure 5.

4 | DISCUSSION

We presented an archival search for overlooked TDEs starting from the more than 8×10^5 detections of the latest XMM-Newton catalogue. Through a blind search, we retrieved four sources that, due to their association with their host galaxy nuclear regions, optical counterpart, luminosity, and spectral shape, are the most convincing TDE candidates.

The spectra of the four TDE candidates are all well modeled by cold blackbody profiles with temperatures $kT \lesssim 100$ eV. This soft X-ray emission is typical of TDEs observed close to their peaks and is consistent, in this scenario, with their observed X-ray luminosities (all above 10^{41} erg/s). Moreover, three of these four sources (T1, T2, and T3) are optically classified as non-active galaxies, favoring a TDE scenario.

Two sources (T2 and T3) have been observed only once by XMM-Newton, so we cannot trace any long-term evolution. We also checked for archival data of other X-ray telescopes, such as ROSAT, Chandra, and Swift, but we found no detection, and we could only infer upper limits above 10^{43} erg/s. A challenging scenario involves the possibility of our sources being HLXs. In this case, these sources would be excellent IMBHs candidates that evaded previous detections due to their proximity to their host galaxy center, as ULXs and HLXs searches usually avoid the galactic central regions (Barrows et al. 2019).

Favoring the TDE scenario, there is also the fact that we asked for a second XMM-Newton observation for the source labeled T1 (PI. Sacchi, Proposal ID: 88474) and we detected it with a flux decreased by a factor ~ 20 with respect to the previous observation.

The fourth source (T4) is peculiar. As the other three sources have an extremely steep X-ray spectrum and, being observed twice by XMM-Newton, show significant long-term variability. In its first observation, it was not detected, while during the second observation, it was detected with a luminosity above 10^{43} erg/s. With respect to the 3σ upper limit of the first observation, this source shows in three years a 400% variability. The optical classification of this source however is that of an AGN due to the presence of broad emission lines. Given these facts, a possible scenario would involve a TDE occurring into

TABLE 1 The quantities in italic are fixed during the fit procedure.

		Blackbody		Powerlaw			Blackbody + Powerlaw			
Lab.	**Date**	C/ν	kT	C/ν	N_H	Γ	C/ν	kT	Γ	$\log_{10} L$
T1	August 8, 2010	**224/234**	$0.062^{+0.004}_{-0.003}$	230/234	*0.0*	$6.1^{+0.4}_{-0.3}$	224/233	$0.063^{+0.004}_{-0.003}$	*3.0*	$41.04^{+0.09}_{-0.10}$
	January 17, 2022									$39.7^{+0.1}_{-0.2}$
T2	November 29, 2006	104/92	$0.11^{+0.01}_{-0.01}$	110/91	$0.14^{+0.1}_{-0.06}$	$5.4^{+1.0}_{-0.7}$	101/89	$0.09^{+0.02}_{-0.02}$	$1.9^{+1.1}_{-0.9}$	$41.33^{+0.12}_{-0.04}$
T3	January 6, 2018	97/95	$0.057^{+0.04}_{-0.005}$	112/95	*0.0*	$6.3^{+0.3}_{-0.3}$	124/93	$0.063^{+0.004}_{-0.005}$	$-0.9^{+0.7}_{-1.0}$	$41.57^{+0.07}_{-0.07}$
T4	October 31, 2009	-	-	-	-	-	-	-	-	*42.56*
	December 3, 2012	51/41	$0.08^{+0.04}_{-0.03}$	70/41	*0.0*	$5.2^{+0.2}_{-0.2}$	45/39	$0.08^{+0.04}_{-0.03}$	$1.0^{+0.6}_{-0.5}$	$43.16^{+0.04}_{-0.04}$

Note: In boldface are the statistics of the best-fitting model. C is the C-statistic, while ν the degrees of freedom. All values are reported with 1σ errors. The blackbody temperature is in keV, the intrinsic absorption hydrogen column density is in 10^{20} atoms/cm^2 units and when *0.0* is indicated, it was fixed to 10^{-5} atoms/cm^2. The intrinsic absorption columns are omitted for the blackbody and blackbody+power law models as no intrinsic absorption was required in any source. The absorbed luminosity, expressed in erg/s, is computed over the 0.5–2 keV range, and adopting the best-fitting model, the luminosity of the first observation of the source labeled T4 is a 3σ upper limit. Best-fitting results are highlighted in boldface.

a pre-existing AGN. A challenging scenario could instead involve some extreme AGN variability phenomena.

A final fact favoring the TDE interpretation for all of the described sources is the efficiency of our method in retrieving known TDEs or very convincing candidates: among the 60 sources composing our parent sample, 9 fall in one of the two mentioned categories. In fact, our algorithm selected 3 more TDEs: OGLE16aaa (Zhang et al. 2016), 3XMM J152130.7+074916 (Lin et al. 2015), and 2XMMi J1847 (Lin et al. 2011), which fully satisfy our luminosity-steepness criterion. However, the redshifts of these TDEs are not listed in optical catalogs and were hence not selected by our method.

We encourage multi-wavelength studies and follow-up observations of the described sources, which will help clarify their nature.

ACKNOWLEDGMENT

Open Access Funding provided by Universita degli Studi di Firenze within the CRUI-CARE Agreement.

ORCID

Andrea Sacchi https://orcid.org/0000-0002-7295-5661

REFERENCES

Ahn, C. P., Alexandroff, R., Allende Prieto, C., et al. 2012, *ApJS*, *203*(2), 21.

Ahumada, R., Allende Prieto, C., Almeida, A. et al. 2019, arXiv e-prints, arXiv:1912.02905.

Bär, R. E., Weigel, A. K., Sartori, L. F., Oh, K., Koss, M., & Schawinski, K. 2017, *MNRAS*, *466*(3), 2879.

Barrows, R. S., Mezcua, M., & Comerford, J. M. 2019, *ApJ*, *882*(2), 181.

Boller, T., Brandt, W. N., Fabian, A. C., & Fink, H. H. 1997, *MNRAS*, *289*(2), 393.

Boller, T., Fabian, A. C., Sunyaev, R., et al. 2002, *MNRAS*, *329*(1), L1.

Castangia, P., Panessa, F., Henkel, C., Kadler, M., & Tarchi, A. 2013, *MNRAS*, *436*(4), 3388.

Colless, M., Peterson, B. A., Jackson, C. et al. 2003, arXiv e-prints, astro-ph/0306581.

Driver, S. P., Hill, D. T., Kelvin, L. S., et al. 2011, *MNRAS*, *413*(2), 971.

Esquej, P., Page, M., Carrera, F. J., et al. 2013, *A&A*, *557*, A123.

Esquej, P., Saxton, R. D., Freyberg, M. J., Read, A. M., Altieri, B., Sanchez-Portal, M., & Hasinger, G. 2007, *A&A*, *462*(3), L49.

Farrell, S. A., Webb, N. A., Barret, D., Godet, O., & Rodrigues, J. M. 2009, *Nature*, *460*(7251), 73.

GierliiIski, M., Middleton, M., Ward, M., & Done, C. 2008, *Nature*, *455*(7211), 369.

Giustini, M., Miniutti, G., & Saxton, R. D. 2020, *A&A*, *636*, L2.

Holoien, T. W.-S., Kochanek, C. S., Prieto, J. L., et al. 2016, *MNRAS*, *455*, 2918.

Jones, D. H., Read, M. A., Saunders, W., et al. 2009, *MNRAS*, *399*(2), 683.

Kaaret, P., Feng, H., & Roberts, T. P. 2017, *ARA&A*, *55*(1), 303.

Lacy, M., Ridgway, S. E., Gates, E. L., et al. 2013, *ApJS*, *208*(2), 24.

LaMassa, S. M., Heckman, T. M., & Ptak, A. 2012, *ApJ*, *758*(2), 82.

Lavaux, G., & Hudson, M. J. 2011, *MNRAS*, *416*(4), 2840.

Lidman, C., Ardila, F., Owers, M., et al. 2016, *PASA*, *33*, e001.

Lin, D., Carrasco, E. R., Grupe, D., Webb, N. A., Barret, D., & Farrell, S. A. 2011, *ApJ*, *738*(1), 52.

Lin, D., Carrasco, E. R., Webb, N. A., et al. 2016, *ApJ*, *821*(1), 25.

Lin, D., Godet, O., Ho, L. C., Barret, D., Webb, N. A., & Irwin, J. A. 2017, *MNRAS*, *468*(1), 783.

Lin, D., Guillochon, J., Komossa, S., et al. 2017, *Nat. Astron.*, *1*, 33.

Lin, D., Irwin, J. A., Godet, O., Webb, N. A., & Barret, D. 2013, *ApJ*, *776*(1), L10.

Lin, D., Maksym, P. W., Irwin, J. A., et al. 2015, *ApJ*, *811*(1), 43.

Liske, J., Baldry, I. K., Driver, S. P., et al. 2015, *MNRAS*, *452*(2), 2087.

Maksym, W. P., Miller, J. M., Cenko, S. B., et al. 2014, *The Astronomer's Telegram*, *6834*, 1.

Mallick, L., & Dewangan, G. C. 2018, *ApJ*, *863*(2), 178.

Menzel, M. L., Merloni, A., Georgakakis, A., et al. 2016, *MNRAS*, *457*(1), 110.

Mickaelian, A. M., Harutyunyan, G. S., & Sarkissian, A. 2018, *Astron. Lett.*, *44*(6), 351.

Miniutti, G., Fabian, A. C., Brandt, W. N., Gallo, L. C., & Boller, T. 2009, *MNRAS*, *396*(1), L85.

Miniutti, G., Saxton, R. D., Giustini, M., et al. 2019, *Nature*, *573*(7774), 381.

Miniutti, G., Saxton, R. D., Rodríguez-Pascual, P. M., et al. 2013, *MNRAS*, *433*(2), 1764.

Pâris, I., Petitjean, P., Aubourg, É., et al. 2018, *A&A*, *613*, A51.

Paturel, G., Petit, C., Prugniel, P., et al. 2003, *A&A*, *412*, 45.

Phinney, E. S. 1989, in: *Manifestations of a Massive Black Hole in the Galactic Center*, ed. M. Morris, Vol. *136*, The Center of the Galaxy, 543.

Pierre, M., Pacaud, F., Adami, C., et al. 2016, *A&A*, *592*, A1.

Rakshit, S., Stalin, C. S., Chand, H., & Zhang, X.-G. 2017, *ApJS*, *229*(2), 39.

Rees, M. J. 1988, *Nature*, *333*, 523.

Ricci, C., Kara, E., Loewenstein, M., et al. 2020, *ApJ*, *898*(1), L1.

Saxton, R., Komossa, S., Auchettl, K., & Jonker, P. G. 2020, *Space Sci. Rev.*, *216*(5), 85.

Saxton, R. D., Read, A. M., Esquej, P., Komossa, S., Dougherty, S., Rodriguez-Pascual, P., & Barrado, D. 2012, *A&A*, *541*, A106.

Shectman, S. A., Landy, S. D., Oemler, A., Tucker, D. L., Lin, H., Kirshner, R. P., & Schechter, P. L. 1996, *ApJ*, *470*, 172.

Shu, X. W., Wang, S. S., Dou, L. M., Jiang, N., Wang, J. X., & Wang, T. G. 2018, *ApJ*, *857*(2), L16.

Sun, L., Shu, X., & Wang, T. 2013, *ApJ*, *768*(2), 167.

Terashima, Y., Kamizasa, N., Awaki, H., Kubota, A., & Ueda, Y. 2012, *ApJ*, *752*(2), 154.

Toba, Y., Oyabu, S., Matsuhara, H., et al. 2014, *ApJ*, *788*(1), 45.

Véron-Cetty, M. P., & Véron, P. 2010, *A&A*, *518*, A10.

Webb, N. A., Coriat, M., Traulsen, I. et al. 2020, arXiv e-prints, arXiv:2007.02899.

Yoon, J. H., Schawinski, K., Sheen, Y.-K., Ree, C. H., & Yi, S. K. 2008, *ApJS*, *176*(2), 414.

Zhang, W., Yu, W., & Yan, Z. 2016, The Astronomer's Telegram, 8644, 1.

How to cite this article: Sacchi, A., Risaliti, G., & Miniutti, G. 2023, *Astron. Nachr.*, *344*, e220128. https://doi.org/10.1002/asna.20220128